Biomaterials 120 (2017) 11–21

Contents lists available at ScienceDirect

Biomaterials

journal homepage: www.elsevier.com/locate/biomaterials

Fabrication of injectable high strength hydrogel based on 4-arm star PEG for cartilage tissue engineering

Jianqi Wang [a, *], Fengjie Zhang [b, c], Wing Pui Tsang [b, c], Chao Wan [b, c, **], Chi Wu [a, d]

[a] Department of Chemistry, The Chinese University of Hong Kong, Hong Kong SAR, PR China
[b] Key Laboratory for Regenerative Medicine, Ministry of Education, School of Biomedical Sciences, Faculty of Medicine, The Chinese University of Hong Kong, Hong Kong SAR, PR China
[c] School of Biomedical Sciences Core Laboratory, Institute of Stem Cell, Genomics and Translational Research, Shenzhen Research Institute, The Chinese University of Hong Kong, Shenzhen 518057, PR China
[d] Hefei National Laboratory for Physical Sciences at Microsacle, Department of Chemical Physics, University of Science and Technology of China, Hefei 230026, PR China

ARTICLE INFO

Article history:
Received 1 September 2016
Received in revised form
29 November 2016
Accepted 19 December 2016
Available online 20 December 2016

Keywords:
Star PEG
Overlap concentration
Injectable hydrogel
Chondrocyte
Cartilage tissue engineering
Young's modulus

ABSTRACT

Hydrogels prepared from poly(ethylene glycol) (PEG) are widely applied in tissue engineering, especially those derived from a combination of functional multi-arm star PEG and linear crosslinker, with an expectation to form a structurally ideal network. However, the poor mechanical strength still renders their further applications. Here we examined the relationship between the dynamics of the pre-gel solution and the mechanical property of the resultant hydrogel in a system consisting of 4-arm star PEG functionalized with vinyl sulfone and short dithiol crosslinker. A method to prepare mechanically strong hydrogel for cartilage tissue engineering is proposed. It is found that when gelation takes place at the overlap concentration, at which a slow relaxation mode just appears in dynamic light scattering (DLS), the resultant hydrogel has a local maximum compressive strength ~20 MPa, while still keeps ultralow mass concentration and Young's modulus. Chondrocyte-laden hydrogel constructed under this condition was transplanted into the subcutaneous pocket and an osteochondral defect model in SCID mice. The *in vivo* results show that chondrocytes can proliferate and maintain their phenotypes in the hydrogel, with the production of abundant extracellular matrix (ECM) components, formation of typical chondrocyte lacunae structure and increase in Young's modulus over 12 weeks, as indicated by histological, immunohistochemistry, gene expression analyses and mechanical test. Moreover, newly formed hyaline cartilage was observed to be integrated with the host articular cartilage tissue in the defects injected with chondrocytes/hydrogel constructs. The results suggest that this hydrogel is a promising candidate scaffold for cartilage tissue engineering.

1. Introduction

Articular cartilage has very limited self-repair ability due to the absence of innervation and vascularization, as well as the intense extracellular matrix (ECM) which impedes cell migration [1,2]. Trauma caused articular cartilage defect is one of the major difficult clinical situations in sports medicine. Incomplete repair of the defect is associated with formation of fibrocartilage and subsequent degeneration of the adjacent hyaline cartilage. It is important to repair cartilage defect in its initial stage before it further progresses, which would lead to osteoarthritis. Current therapies for articular cartilage repair include micro-fracture of subchondral bone [3], autologous chondrocyte transplantation [4], osteoarticular transfer system [5] and local delivery of hyaluronic acid or glucocorticoid [6]. However, the clinical efficacy of the above therapies remains unsatisfied. Tissue engineering approach emerges as a promising therapy for functional cartilage repair or regeneration [7]. Particularly, the matrix-assisted autologous chondrocyte transplantation (MACT) has achieved great development during the last decade [8,9]. This technique involves the encapsulation of autologous

* Corresponding author. Department of Chemistry, The Chinese University of Hong Kong, Hong Kong SAR, PR China.
** Corresponding author. Key Laboratory for Regenerative Medicine, Ministry of Education, School of Biomedical Sciences, Faculty of Medicine, The Chinese University of Hong Kong, Hong Kong SAR, PR China.
E-mail addresses: agathis.wang@gmail.com (J. Wang), cwan@cuhk.edu.hk (C. Wan).

http://dx.doi.org/10.1016/j.biomaterials.2016.12.015
0142-9612/

chondrocytes into a carefully designed scaffold, in which chondrocytes can proliferate and secret ECM. The whole cell/scaffold construct is then transplanted into the cartilage focal lesion. Various types of materials, both derived from modified natural products and synthetic materials have been examined as the potential scaffold matrix [10–12].

Among the numerous materials, synthetic hydrogel has been one of the most promising candidates due to its high water content, good mass transportation property, soft tissue like elasticity and biocompatibility [13]. It can be well tuned via various chemistries to satisfy the clinical needs. For instance, by using bio-orthogonal chemistry, the injectable hydrogel allows the minimally invasive surgery possible [14–16]. To synchronize the degradation rate of the scaffold with the matrix deposition rate by the encapsulated cells, matrix metalloproteinase (MMP) peptides have been adopted as the crosslinker [2,17–19]. Among the synthetic materials, poly(ethylene glycol) (PEG) has been the most widely used building block for hydrogel. Basically two gelation mechanisms have been employed. The first one involves the chain polymerization of PEG dimethylacrylate [20–23]. Due to the fast kinetics and random crosslinking process, the resulting hydrogel has an irregular structure and a weak mechanical strength. The alternative method uses the step growth polymerization, where functional multiple-arm star PEG reacts with crosslinkers bearing at least two reactive sites, typically using functional 4-arm star PEG and difunctional linear crosslinkers, i.e., 4 + 2 system [17–19,24–30]. This method is expected to result in a much more ideal hydrogel structure comparing to the chain polymerization counterpart [31]. Moreover, it allows the modularization design of functional hydrogel. The incorporation of important biological signals or cues [31,32] and introduction of controlled degradation profile [2,33,34] have been realized by simply varying the functionality of the linear crosslinkers.

However, one major problem has rarely been clarified despite the wide usage of this step growth strategy, i.e., how to achieve the ideal network structure? The hydrogel with ideal network structure is expected to have a high mechanical strength due to the elimination of the structural defects, which would overcome the longstanding major drawback of hydrogel, *viz*., the poor mechanical properties [7,35]. Hydrogel with high strength is more suitable for earlier implantation after the cell/hydrogel hybrid construction, which will help shorten the *in vitro* culture period, and provides sufficient load-bearing capacity for mechanical loading *in vivo* before the secretion of ECM [36]. It will survive from the harsh environment in the diarthrodial joints and be a promising candidate for the MACT. Moreover, the optimization of the hydrogel formulation would also decrease the material dosage and minimize the introduction of exogenous materials.

For the current 4 + 2 system, it is necessary to prepare the hydrogel at a suitable concentration. When the concentration of star polymer is too low, the difunctional crosslinker cannot link them efficiently; when the concentration is too high, there will be penetration and entanglement between the arm chains. The most suitable concentration should be around overlap concentration (C^*), where polymer chains start to touch each other [37]. In this study, we started from an investigation on the dynamics of star PEG in phosphate-buffered saline (PBS) solution at different concentrations with dynamic light scattering (DLS) to find the optimal concentration, given that there would be dynamics change around C^*. After that, we prepared a mechanically strong hydrogel for the cartilage tissue engineering using the 4 + 2 system based on the DLS result. Murine chondrocytes were encapsulated in the hydrogel prepared at this concentration and the resultant chondrocyte/hydrogel constructs were transplanted into severe combined immunodeficiency (SCID) mice up to 12 weeks to allow the engineered cartilage tissue to develop. The cell morphology, ECM synthesis, expression of chondrogenic marker proteins and mechanical properties of the newly formed cartilage tissue derived from the chondrocytes/hydrogel constructs were examined. At last, an osteochondral defect model in SCID mice was performed and the capacity of cartilage defect repair was tested.

2. Materials and methods

2.1. Materials

Ethylene oxide was purchased from Hong Kong Specialty Gases, HK. Potassium, naphthalene, diphenyl methane, pentaerythritol, anhydrous DMSO, divinyl sulfone, sodium hydride, acetic acid and 2, 2'-(ethylenedioxy) diethanethiol were purchased from Sigma-Aldrich, US. 4-arm star PEG (M_n = 1.6 × 10^4 g/mol, PDI = 1.03) was synthesized according to Wang et al. by high vacuum living anionic polymerization of ethylene oxide in a home-designed glassware using pentaerythritol as the initiator and diphenyl methyl potassium as the deprotonating agent [38].

2.2. Synthesis of star PEG vinyl sulfone (sPEG-VS)

*s*PEG-VS was synthesized by coupling *s*PEG-OH with an excess of divinyl sulfone following the procedure by Lutolf et al. [39]. *s*PEG-OH was dried by azeotropic distillation in toluene using a Dean Stark trap before starting the reaction. To the *s*PEG-OH dissolved in anhydrous dichloromethane, NaH was added under nitrogen at 5-fold molar excess over OH group. After hydrogen evolution, the suspension was added dropwisely to a solution of divinyl sulfone in anhydrous dichloromethane via syringe. The reaction was carried out at room temperature for 3 days in dark under nitrogen atmosphere. After the reaction solution being neutralized with acetic acid, filtered through celite and concentrated, the product was recovered by repeated precipitation in cold diethyl ether and dried in vacuum. The degree of end modification was checked by ^{1}HNMR and found to be quantitative. ^{1}HNMR ($CDCl_3$): δ = 3.2–3.3 (−O−*CH*$_2$−CH_2−SO_2−), δ = 3.41 (−C−*CH*$_2$O−), δ = 3.6–3.7 (−O−*CH*$_2$−*CH*$_2$−O), δ = 3.8–3.9 (−O−CH_2−*CH*$_2$−SO_2−), δ = 6.07–6.10 (*CH*$_2$=CH−), δ = 6.37–6.41 (*CH*$_2$=CH−), δ = 6.79–6.85 (CH_2=*CH*−).

2.3. Experimental determination of overlap concentration

Dynamics of the 4-arm star PEG in PBS solution was studied by DLS on a commercial LLS spectrometer (ALV/DLS/SLS-5022F) equipped with a multi-τ digital time correlator (ALV5000) and a vertically polarized 22 mW He−Ne cylindrical laser (λ_0 = 632.8 nm, Uniphase). The details on the light scattering instrumentation, theory and data treatment can be found elsewhere [40–44]. The star PEG PBS solutions were pre-treated by repeated filtration through a 0.45 μm hydrophilic PTFE filter to remove the nanobubbles stabilized by the PEG chains, which would result in an apparent slow mode in the dilute solution regime [45–47]. The corresponding correlation function was resolved by CONTIN program provided by ALV. The diffusion coefficient (D) of the star PEG in PBS solution at every concentration was determined from $\Gamma = Dq^2$, where Γ is the line-width obtained from the CONTIN analysis and q is the scattering vector.

2.4. Isolation and culture of murine chondrocytes

Murine chondrocytes isolation and culture were performed following established method [48,49]. Briefly, primary chondrocytes were isolated from the ribs of C57BL/6 new-born mice

euthanized by cervical dislocation. The ribs were digested by collagenase I and collagenase D (Worthington, Worthington Biochemical Co.) and chondrocytes were plated onto a 100 mm Petri dish with DMEM (Gibco, Invitrogen) supplemented with 1% penicillin/streptomycin sulfate (P/S) (Gibco, Invitrogen), 1% L-glutamine (Gibco, Invitrogen) and 10% fetal bovine serum (FBS) (Gibco, Invitrogen) at 37 °C in a 5% CO_2 humidified incubator. On the second day, non-adherent cells were sucked out and the cultures were gently rinsed with PBS twice and cultured in fresh normal culture medium (DMEM containing 10% FBS, 1% P/S and 1% L-glutamine). The adherent cells were cultured and the medium was changed every 2 days until the cells became confluent. The second passage cells were used for the chondrocytes/hydrogel construction.

2.5. Hydrogel formulation and cell encapsulation

*s*PEG-VS and 2,2'-(ethylenedioxy) diethanethiol were dissolved in PBS separately with the same molar concentration of vinyl sulfone group and thiol group. Equal volume of the above two solutions were mixed to fabricate the hydrogel at different concentrations in a 1 mL syringe mold with cut head.

For the acellular experiment, the crosslinking reaction was allowed to proceed overnight at 37 °C before the mechanical property measurement on the newly generated hydrogel scaffold. For the cell encapsulation experiment, all the solutions were sterilized via filtration through sterilized disposable 0.22 μm syringe filter (Millipore, US) in the biosafety cabinet. The chondrocytes were suspended at a density of 4×10^7 cells/mL and the resulting chondrocytes/pre-hydrogel suspensions were injected into sterilized disposable 1 mL syringe molds and incubated at 37 °C for 1 h in a 5% CO_2 humidified incubator for gelation. The result chondrocytes/hydrogel constructs (~20 μL) were then transferred to 12-well culture plates and incubated in the normal culture medium overnight for further gelation before subcutaneous transplantation into the SCID mice.

2.6. Mechanical property measurement of hydrogel

The compression test of the hydrogel without cell was carried out on a mechanical testing apparatus (MTS QT/1L, MTS Systems Corporation, US.) at a velocity of 1 mm/min. For the cell-laden hydrogel, the compressive Young's modulus was measured on a Mach-1 mechanical testing system (Biomomentum Inc. Canada) at a velocity of 20% height/min until a strain of 30%. The corresponding compressive modulus was estimated from the slop of the linear region of the stress-strain curve following previous protocol [2].

2.7. In vivo subcutaneous transplantation of chondrocytes/hydrogel constructs

In vivo experimental procedure was carried out according to protocols approved by Animal Experimentation Ethics Committee, The Chinese University of Hong Kong and Animal (Control of Experiments) Ordinance from Department of Health, Hong Kong SAR. For subcutaneous transplantation, 4-week old male SCID mice were anesthetized using Xylazine (Sigma-Aldrich, 5 mg/kg) and Ketamine (Alfasan, Holland, 40 mg/kg) cocktail under sterile conditions. The chondrocytes/hydrogel constructs were transplanted into subcutaneous pockets created by blunt dissection following a 5 mm long skin incision on the back of the SCID mice. The skin wounds were carefully closed with standard surgical procedure. The mice were sacrificed by cervical dislocation and the samples were collected after the time of interest.

2.8. Articular cartilage repair in mouse osteochondral defect model

The mouse osteochondral defect model was adapted from established protocol [50]. Briefly, 8-week old SCID mice (20–25 g) were anesthetized using Xylazine (5 mg/kg) and Ketamine (40 mg/kg) cocktail. Under sterile conditions, the inter-condyle notch of the left distal femur was exposed and an osteochondral defect with 1 mm in diameter and 1 mm in depth was created with a fine surgical drill. The defects were injected with 1 μL chondrocytes/pre-hydrogel suspension (cell number ~ 1×10^5), with non-treatment as control. Five mice were used in each group. Gelation occurred within 5–10 min. The wounds were then carefully sewed up with standard surgical procedure. After surgery, the animals were administered with analgesics (Buprenorphine HCl, 0.02 mg/kg/day) once per day for three days. The animals were monitored every day post-surgery in the first week. At 6 and 12 weeks post-surgery, the animals were sacrificed by cervical dislocation. The cartilage samples of the distal femur were harvested, fixed with 4% paraformaldehyde (PFA) solution, decalcified with 10% EDTA solution for 2 weeks at 4 °C and further processed for Safranin O staining.

2.9. Histological and immunohistochemistry analysis

The harvested samples were fixed with 4% PFA solution for 12 h at 4 °C, filtrated with O.C.T. Compound (Sakura Finetek, US) and cryo-sectioned on a cryotome (Thermo Scientific, US) as previously described [51]. Sections with a thickness of 10 μm were collected on SuperFrost® Plus Gold slides (Fisher Scientific, US), dried in air and stained with Alcian blue, Safranin O, Sirius red and Masson's trichrome to visualize and evaluate the ECM production.

Dako EnVision™ visualization kit (Agilent Technologies, US) was used for immunohistochemistry analysis following manufacturer's instruction. Sections were blocked with dual endogenous enzyme block for 15 min, and further incubated with antibodies against collagen type II (Col II) (Abcam, 1:100) or Sox 9 (Abcam, 1:100). Sections incubated with 1% non-immune IgG solution were served as negative controls. All samples were processed at the same time to minimize sample-to-sample variation. All the images were analyzed and quantified by ImageJ software.

2.10. Quantitative real-time PCR

Total RNA was extracted using the RNeasy Mini Kit (Qiagen). First strand cDNA was synthesized from 0.5 μg total RNA in the presence of oligo-$dT_{12\text{-}18}$ primer (Invitrogen) and 200 units of MMLV reverse transcriptase according to manufacturer's protocol (Promega). Quantitative real-time PCR was performed using the SYBR Premix Ex Taq (Takara) in ABI Fast Real-time PCR 7900HT System (Applied Biosystems). Each reaction was performed in triplicates under the following parameters: 95 °C for 30s and 40 cycles of 95 °C for 10s. Target mRNA levels were normalized to β-actin expression.

3. Results and discussion

For the above 4 + 2 system, a majority of the previous work on the design of the hydrogel scaffold for tissue engineering has been focused on the functionalization of the scaffold, such as the cross-linking chemistry, the degradation profile, the incorporation of bioactive factors and stimuli-responsibility. Optimization on the network structure of the hydrogel has frequently been overlooked, especially the effect of the mass concentration of the hydrogelator. The mass concentration used in the hydrogel formulation is

frequently determined through trials and errors. No extract guidelines have ever been proposed on this issue.

Previous simulation results revealed that the arm chains in a star polymer adopt more elongated conformation than the random coil in good solvent in the low molecular weight limit, which endows the 4-arm star polymer a tetrahedron like structure [52,53]. Moreover, star polymer exhibits osmotic repulsion due to its inhomogeneous monomer density distribution, leading to ordering phenomena in the vicinity of C^* [54,55], where polymer chains start to touch each other. It is natural to expect that if 4-arm star polymer chains are interconnected at C^* with a short linear crosslinker, the resultant hydrogel network structure would be an analogue to the crystal structure of diamond, as illustrated in Scheme 1. The lateral is known for its hardness.

3.1. Overlap concentration of star PEG in aqueous solution

Principally, C^* can be determined as $3M_w/(4\pi N_A R_g^3)$ or $M_w/(2^{3/2}\pi N_A R_g^3)$ or $[\eta]^{-1}$, where M_w, R_g, N_A, $[\eta]$ are the molar mass, the radius of gyration, the Avogadro's constant and the intrinsic viscosity, respectively [56–58]. Note that these definitions are not identical and the difference of C^* calculated from them could be as large as five times [59]. On the other hand, the dynamics is expected to behave differently when the concentration exceeds C^* due to the chain overlapping and entanglement. Chu et al. ever pointed out that bimodal relaxation behavior could be observed in DLS in the crossover regime from the dilute to the semidilute polymer solution [60,61]. Furthermore, Huber et al. observed a bimodal relaxation behavior in the semidilute regime of 12-arm star polystyrene toluene solution and suggested to use the onset concentration of the bimodal relaxation behavior as C^* [62]. Recently, our group also observed the appearance of the slow mode in the vicinity of C^* in 4-arm star polystyrene cyclohexane solution [63]. Based on the previous experimental results, it is reasonable to view the appearance of the slow mode as the arrival of C^* in the polymer solution. Thus, we decided to determine the C^* experimentally by investigating the dynamics of star PEG in PBS solution at different concentrations via DLS, from dilute to semidilute regime. It is found that there is only one relaxation mode when $C < 40$ mg/mL, which is originated from the translational diffusion of individual star PEG chains. A second, namely slow relaxation mode, which is 2–3 orders slower than the translational diffusion appears when $C = 40$ mg/mL. The crossover of the relaxation behavior in DLS is shown in Fig. 1A, indicated by both the normalized intensity-intensity correlation function and the corresponding decay time distribution. Moreover, the concentration at which the slow mode just appears is coupled with the turning point in the diffusion coefficient of the fast mode *vs*. concentration plot ($D \sim C$ plot, Fig. 1B). After the concentration reaching 40 mg/mL, the concentration dependence of the diffusion coefficient of the fast mode starts to deviate from that in the range of 20–35 mg/mL, which is indicated and extrapolated by the dash line. This turning point in the $D \sim C$ plot is caused by the switch of the scattering objects. Before the turning point, the diffusion coefficient is a measurement of the translational diffusion of the whole individual star PEG chain as mentioned above. After that, it is a reflection of the cooperative diffusion of partial short chain segments ("blobs"), whose sizes decrease with increasing concentration as demonstrated by the scaling theory proposed by de Gennes et al. [37,64]. The two DLS results indicate that at $C = 40$ mg/mL, the star PEG chains began to touch each other, i.e., the solution just entered the semidilute regime. This concentration was determined as C^* in this study.

3.2. Mechanical properties of hydrogel

Model hydrogel was fabricated via the Michael addition reaction between the vinyl sulfone and thiol group for its high efficiency and mild reaction condition, as shown in Scheme 1. The reaction can proceed in physiological condition and does not require any external stimulation, which makes the current system biocompatible and injectable. *s*PEG-VS was successfully synthesized via the well-established method with quantitative conversion. A commercially available small molecule, 2, 2'-(ethylenedioxy) diethanethiol, was adopted as the model short linear crosslinker. Here, the use of small molecule crosslinker could facilitate the mixing process with functionalized star PEG and avoid possible chain entanglement with the star polymer. Gelation took place in PBS solution within minutes at 37 °C with a stoichiometric balance between the vinyl sulfone group and thiol group. The network

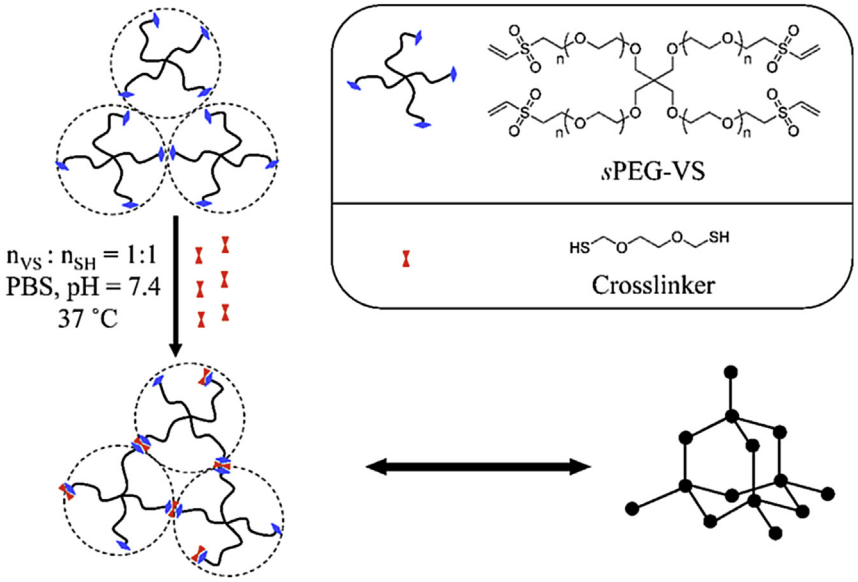

Scheme 1. Fabrication of hydrogel with ideal network structure.

ideality was examined by evaluating the compressive mechanical strength of the resulting hydrogel. The breaking stress of the hydrogel shows a concentration dependence and reaches a local maximum at the previously determined overlap concentration, as shown in Fig. 2A, which supports our speculation. Similar phenomenon where local maximum compressive strength appears around C^* (determined by the viscosity measurement) has also been observed by Sakai et al. [53] in a 4 + 4 system, where 4-arm star PEG functionalized with activated acid and 4-arm star PEG of equal molar mass functionalized with amine group reacted with each other to form the hydrogel.

The breaking stress of the hydrogel prepared at the overlap concentration reaches ~20 MPa, much larger than the traditional hydrogel formed by physical crosslinking (e.g. agarose hydrogel, ~0.1 MPa) or randomly chemical crosslinking (e.g. polyacrylamide hydrogel, ~1 MPa) with the same mass concentration, as shown in Fig. 2B. The breaking stress of the current hydrogel also exceeds the stress that natural cartilage would experience in human body, ranging from 5 to 10 MPa [65,66]. It should be noted that this high mechanical strength was achieved at a mass concentration ~4%, much lower than the frequently used polymer mass concentration range (10–40%) [17,24,28].

Despite the high mechanical strength, the current hydrogel has a very low Young's modulus (~6 kPa) at low strain. Previous work demonstrated that a low modulus can help to maintain the phenotype of the chondrocytes and facilitate the synthesis of ECM [19,67]. Cartilage is a mechanically complex and heterogeneous tissue [68]. The local stiffness of the pericellular matrix (PCM), i.e., the ECM closest to chondrocytes, is significantly lower than the bulk cartilage in adult tissue [67,69–72]. Thus, it is essential for the hydrogel scaffold used for the MACT to be soft enough. Moreover, the softness of the hydrogel allows more space for the proliferation of the chondrocytes during the *in vivo* incubation. The high mechanical strength and the ultralow Young's modulus make the current hydrogel an ideal candidate for the MACT or cartilage tissue engineering.

3.3. Chondrocyte viability and proliferation in subcutaneous transplantation model

The chondrocyte cell density in the hydrogel was determined by quantitative analysis based on the anti-Sox9 immunohistochemistry staining on the frozen sections of the chondrocytes/hydrogel constructs following subcutaneous transplantation in the SCID mice. Sox9 is identified as the key transcription factor controlling

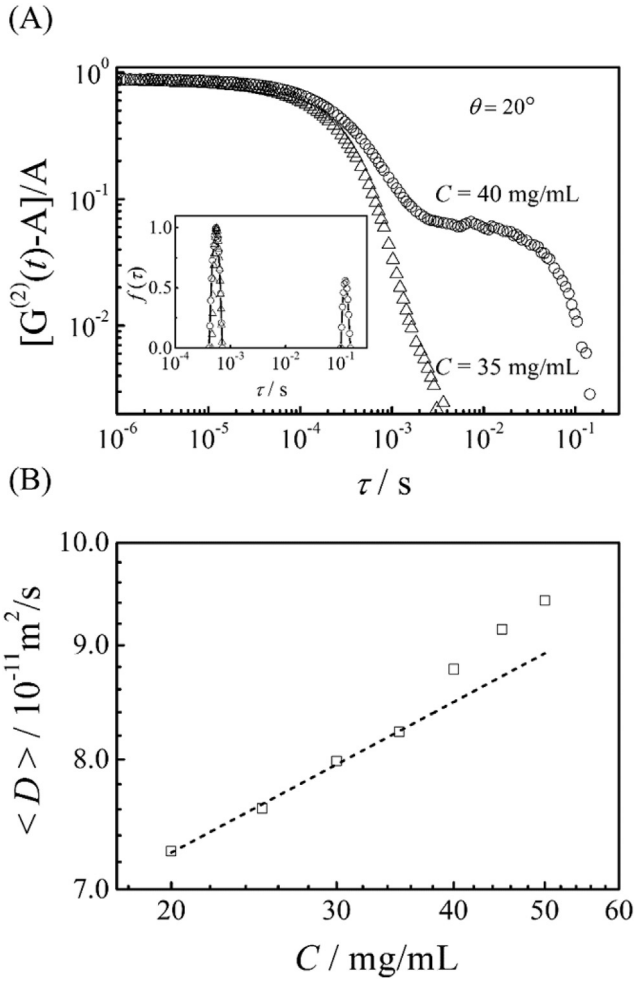

Fig. 1. (A) Concentration dependence of the normalized intensity-intensity correlation function of 4-arm star PEG in PBS solution in the transition zone. The inset shows the corresponding decay time distribution. (B) Concentration dependence of the diffusion coefficient of the fast mode of 4-arm star PEG in PBS solution. The diffusion coefficients in dilute solution regime were connected and extrapolated by a dash line for guidance. $T = 25$ °C.

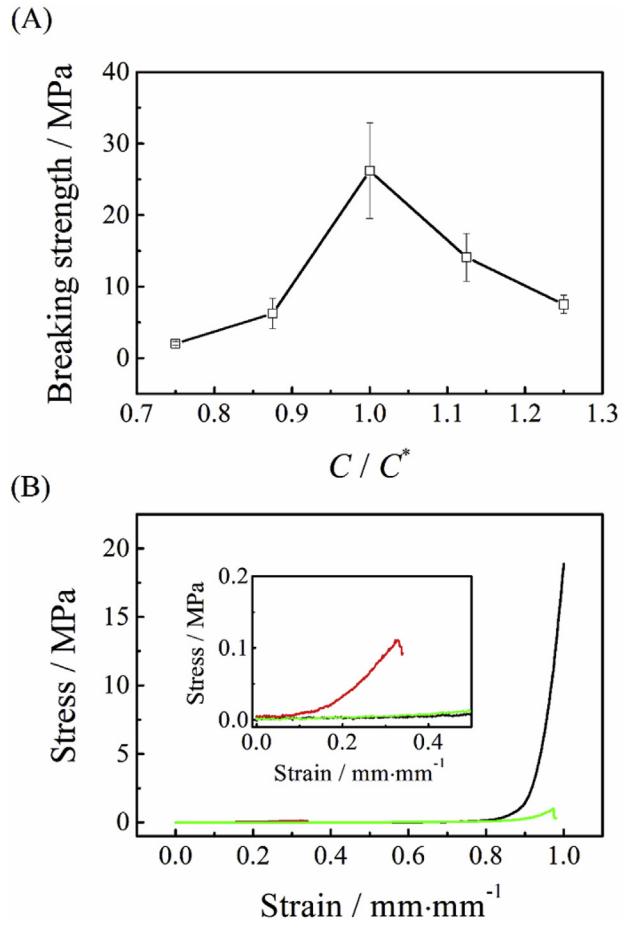

Fig. 2. (A) Concentration dependence of the breaking compressive stress of the star PEG hydrogel (measured in triplicates), where $C^* = 40$ mg/mL. (B) Typical strain-stress curves of three types of hydrogel at the same mass concentration (4%), including the current (black), agarose (red) and polyacrylamide (green) hydrogel. The inset shows the low strain stage to better illustrate the mechanical properties of agarose hydrogel. (For interpretation of the references to colour in this figure legend, the reader is referred to the web version of this article.)

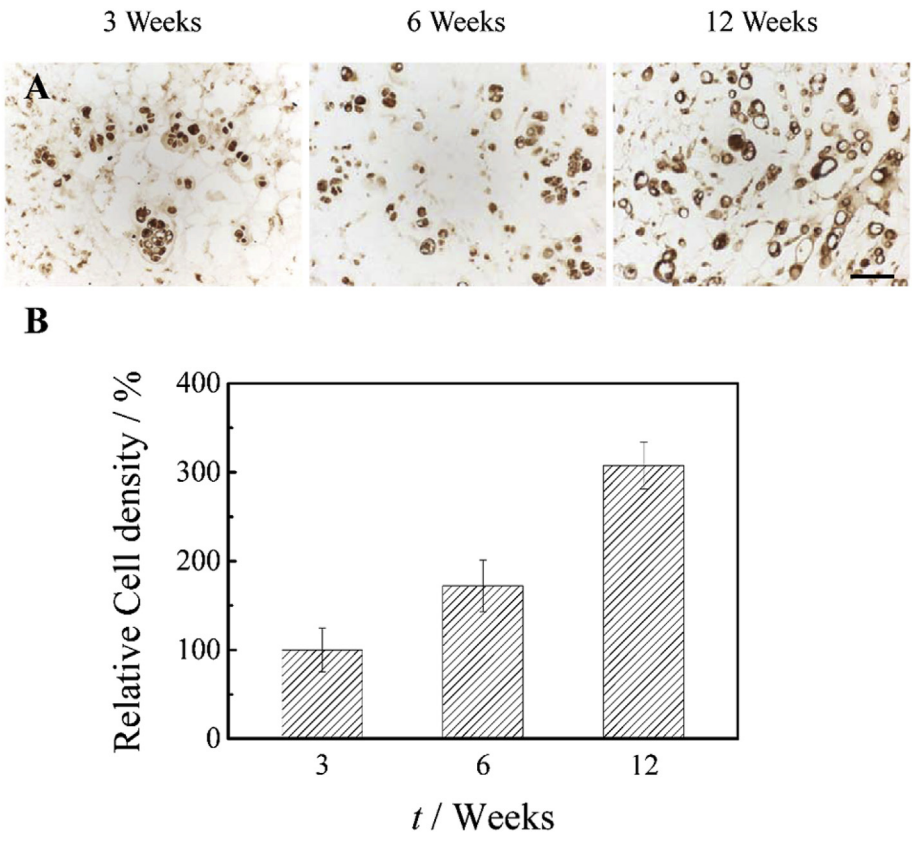

Fig. 3. The relative cell density in the chondrocytes/hydrogel constructs at indicated time points over 12 weeks. (A) Representative images of immunostaining against Sox9 in frozen sections of chondrocytes/hydrogel constructs at 3, 6 and 12 weeks post-surgery. Scale bar: 100 μm. (B) Quantitation of relative chondrocyte cell density from samples harvested at indicated time points.

chondrocyte differentiation [73], which selectively marks the nuclei of the chondrocytes in the newly formed engineered cartilage tissue. A constant increase in the cell density was observed during the 12 weeks *in vivo* subcutaneous incubation as shown in Fig. 3, indicating the excellent cell compatibility, proliferation capability and chondrogenic differentiation potential within the hydrogel.

3.4. Chondrogenic marker genes expression in subcutaneous transplantation model

To examine the phenotype of chondrogensis in the chondrocytes/hydrogel constructs *in vivo*, total RNA was extracted and subjected to quantitative real-time PCR to detect the mRNA expression of chondrogenic markers. As indicated in Fig. 4, a remarkable upregulation of Sox9, Col2a1 and Aggrecan mRNA was observed at 6 weeks post-subcutaneous transplantation. The results suggest that transplanted cells were efficiently differentiated into active chondrocytes within the hydrogel matrix. However, the above marker gene expression was downregulated following further incubation up to 12 weeks *in vivo*. The results indicate that the chondrogenic differentiation in the hydrogel matrix is a dynamic process that coordinates chondrocyte proliferation and maturation.

3.5. ECM production by chondrocytes in subcutaneous transplantation model

It is the ECM components produced by the chondrocytes, mainly glycosaminoglycan and Col II, that endow the cartilage

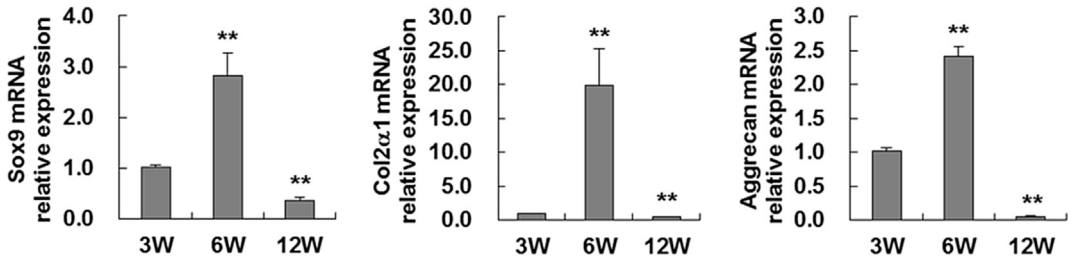

Fig. 4. The mRNA expression of chondrogenic markers (Sox9, Col2α1, Aggrecan) detected by quantitative real-time PCR at indicated time points. The mRNA levels were normalized to the β-actin levels. Data shown are Means ± SD from three independent experiments. *, $P < 0.05$; **, $P < 0.01$.

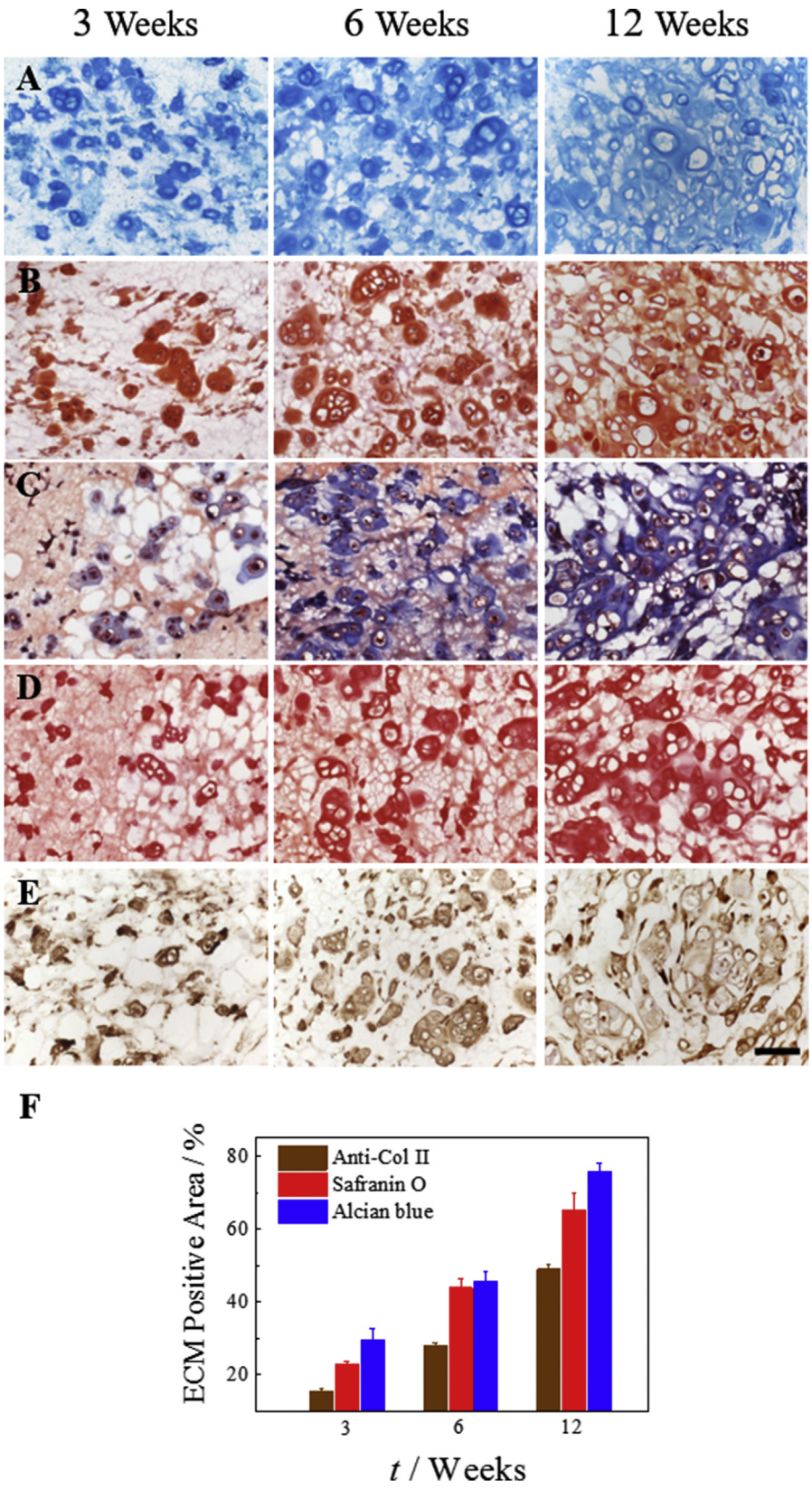

Fig. 5. ECM components production at different time points in the chondrocytes/hydrogel constructs over 12 weeks. Shown are representative images of Alcian blue staining (A); Safranin O staining (B); Mason's trichrome staining (C); Sirius red staining (D); Anti-Col II immunohistochemistry staining (E) on frozen sections of chondrocytes/hydrogel constructs at indicated time points; (F) ECM components production in the chondrocytes/hydrogel constructs over 12 weeks determined by different staining methods indexed by percentage of ECM positive area. Scale bar: 100 μm.

with unique mechanical properties. The phenotypic maintenance of chondrocytes and expression of cellular functions in chondrocytes/hydrogel matrix are key issues for the cartilage engineering and regeneration of neocartilage [74]. Various ECM components were analyzed by the histochemistry staining methods including Alcian blue staining to indicate the glycosaminoglycan, Safranin O staining to index proteoglycan, Sirius red and Masson's trichrome staining to characterize total collagen, and immunohistochemistry staining for Col II specifically to define the cartilage phenotype, as shown in Fig. 5A–E. The positive staining area in each method was determined by the image analysis and summarized in Fig. 5F.

It is clearly shown in the staining result that the chondrocytes keep a spherical morphology, instead of the commonly spindle-like morphology in the 2D cell culture [11]. The spherical morphology with lacuna structure is a typical feature of the chondrocyte phenotype in mature cartilage. The maintenance of the chondrocyte phenotypes allows the production of ECM for the formation of neocartilage. A constant increase in the production of ECM from 3 weeks to 12 weeks was observed by the histochemistry and immunohistochemistry analysis on the sections of newly formed engineered cartilage tissue. Moreover, the texture of stained area evolved from discrete island-like to an interconnected network-like. The evolution indicates that the ECM produced by the chondrocytes diffused from the pericellular space to more global area to form an integrated cartilage tissue.

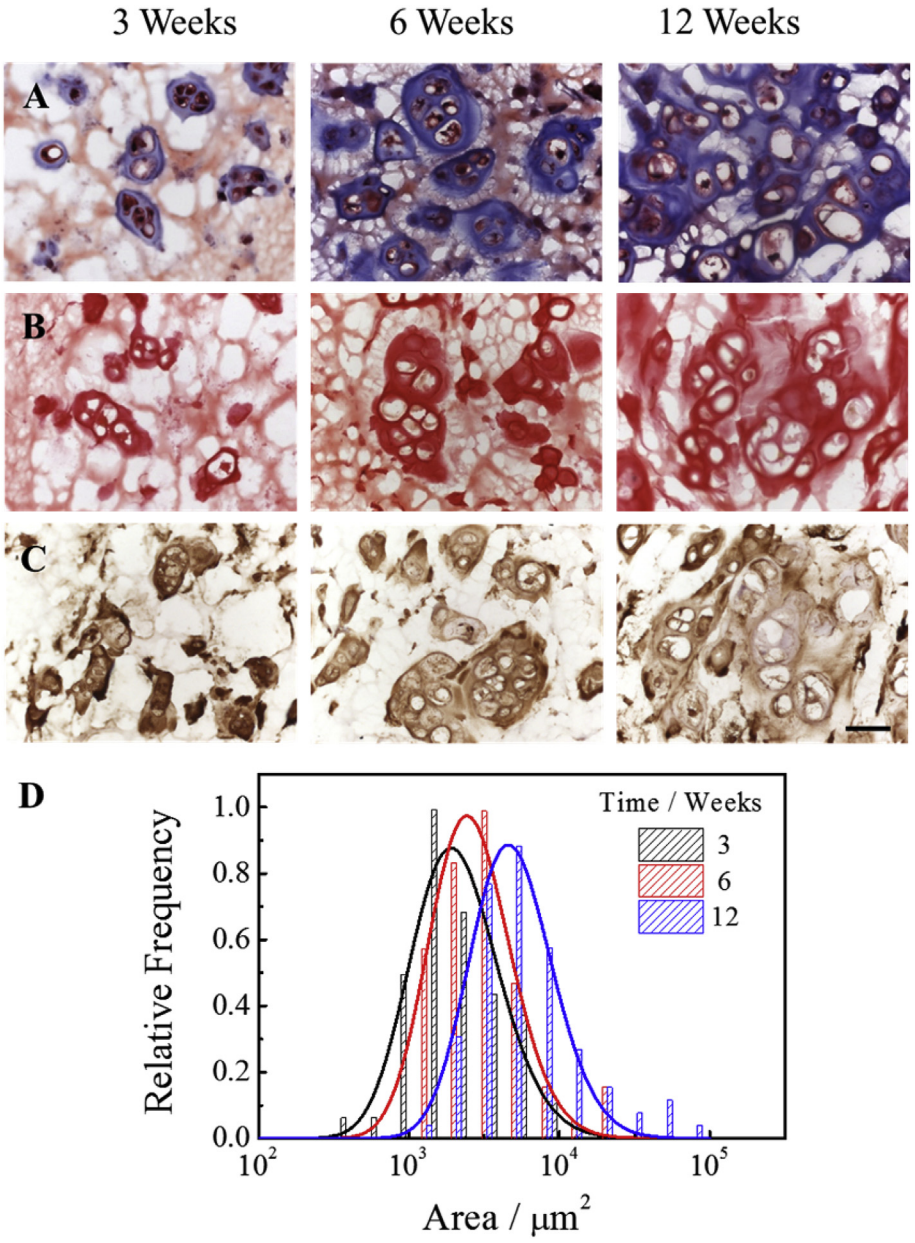

Fig. 6. The size of chondrocyte colony structures formed in the chondrocytes/hydrogel constructs at different time points over 12 weeks visualized by Masson's trichrome (A), Sirius red (B) and anti-Col II immunohistochemistry staining (C) and its analytical result calculated with ImageJ based on the anti-Col II staining result (D). The solid lines are fitting curves by the Log-Normal distribution. Scale bar: 50 μm.

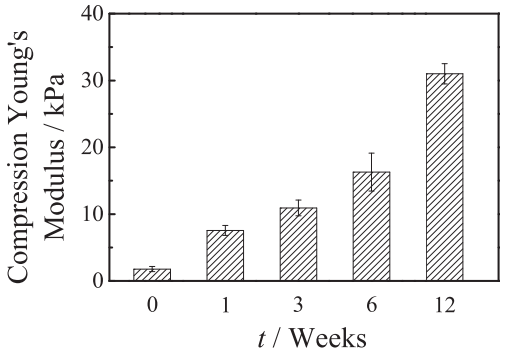

Fig. 7. The compressive Young's modulus of the chondrocytes/hydrogel constructs determined from the strain-stress curves at indicated time points over 12 weeks.

3.6. Evolution of the size of chondrocyte colony and the formation of lacuna structures in subcutaneous transplantation model

As a result of the proliferation of chondrocytes and the secretion of ECM, abundant cell colonies, where several chondrocytes closely aggregate and are surrounded by rich ECM components, were formed in the chondrocytes/hydrogel constructs during the 12 weeks subcutaneous incubation as indicated by the staining result in Fig. 6A–C. The area of the chondrocyte colony was calculated and fitted with a Log-Normal distribution based on the anti-Col II immunostaining result as shown in Fig. 6D. A significant increase in the size of the colony structure was observed over 12 weeks, as indicated by the peak shift towards the larger area in Fig. 6D. This closely packed chondrocyte structure has positive influence on the secretion of ECM. Chondrocytes in the natural cartilage live in hypoxic environment and the formation of such colony structure will limit the exposure of individual cells to the environmental oxygen, thereby enhancing the chondrogenic capacity of chondrocytes and inhibiting dedifferentiation in the hydrogel matrix [75–77]. Moreover, pockets of space around the cells were observed, with a similar morphology to the lacunae typically observed in the cartilage tissue. Its appearance is indicative of neocartilage formation.

3.7. Evolution of Young's modulus of chondrocytes/hydrogel constructs in subcutaneous transplantation model

To confirm the chondrocytes encapsulated in the current hydrogel produced functional, cartilage-specific matrix molecules and they resulted in a structure with increased mechanical properties over time, we assessed the bulk compressive modulus of the cell-laden constructs at different time intervals and the results are summarized in Fig. 7. The bulk Young's modulus increased from the initial ~1 kPa—~30 kPa over 12 weeks. The constant increase in the Young's modulus indicates that the produced ECM has been assembled in an appropriate fashion to stiffen the strength of the scaffold [2], subsequently facilitated the generation of functional cartilage tissue with mechanical durability.

3.8. Articular cartilage repair in the osteochondral defect model

After confirming the chondrocytes/hydrogel constructs can develop into cartilagenous tissue in the subcutaneous pocket, its capacity on articular cartilage repair was further examined. Chondrocytes/pre-hydrogel suspensions were injected into osteochondral defects in mice with non-treatment as control. At 6 weeks post-surgery, the osteochondral defects were partially filled with Safranin O positive stained cartilagenous tissue in the chondrocytes/hydrogel constructs transplanted group (Fig. 8B), while only amorphous mesenchymal tissue and newly formed subchondral bone were observed in the defect region of the control group (Fig. 8A). At 12 weeks post-surgery, high amount of hyaline cartilage was observed to be integrated with the host articular cartilage tissue (Fig. 8D). However, only thin layer of less mature cartilaginous tissue and subchondral bone were observed in the control group (Fig. 8C).

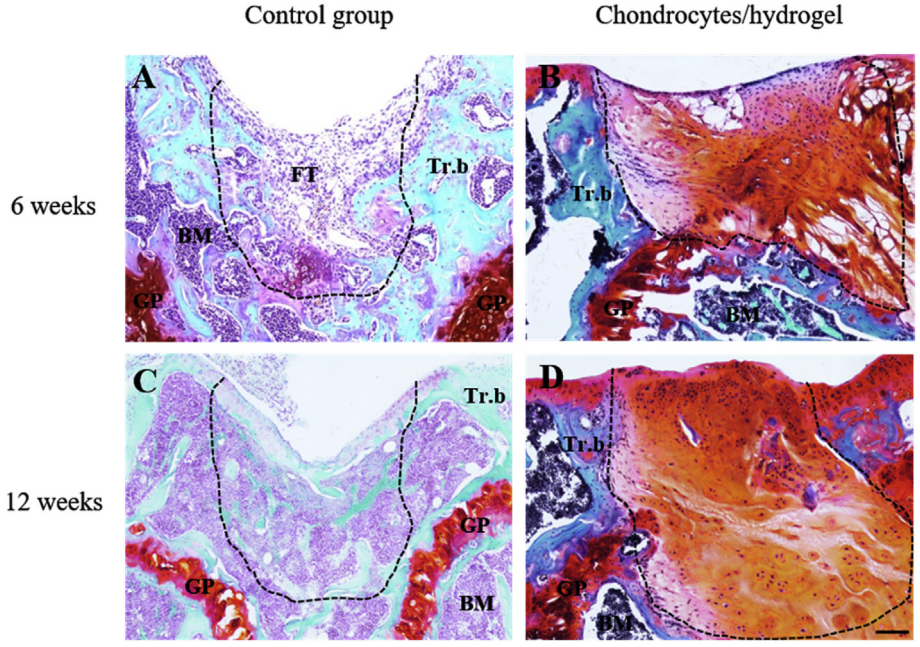

Fig. 8. Articular cartilage repair enhanced by chondrocytes/hydrogel constructs in mouse osteochondral defect model over 12 weeks. Shown are representative images of Safranin O staining on frozen sections in the osteochondral defect model at 6 weeks (A, B) and 12 weeks (C, D) post-surgery, with non-treatment as control. The dash lines indicate the newly formed tissue in the osteochondral defect region. BM, bone marrow; FT, fibrous tissue; GP, growth plate; Tr.b, trabecular bone. Scale bar: 100 μm.

The data provide proof of principle that the resultant hydrogel possesses excellent capacity for articular cartilage repair using tissue engineering approach. However, we could not rule out the integration between the newly formed articular cartilage and subchondral bone, which deserves further investigation.

4. Conclusion

In the present study, a guideline for preparing hydrogel with ideal network structure based on the 4 + 2 system was established by a combination of dynamics and mechanical property study. The key issue is to conduct gelation at the overlap concentration of the 4-arm star polymer, at which a slow mode just appears in DLS spectrum, with a short dithiol crosslinker. An injectable mechanically strong hydrogel with a strength (~20 MPa) comparable to that of natural cartilage while still keeping a very low Young's modulus (~6 kPa) was fabricated at an ultralow mass concentration (4%) following this guideline. Chondrocytes were encapsulated in the hydrogel and *in vivo* subcutaneous culture up to 12 weeks in SCID mice was performed first. It is found that the chondrocytes encapsulated could proliferate and preserve their phenotypes, leading to the production of abundant ECM within the hydrogel during the experimental time window. ECM components including proteoglycan and Col II were identified to be comparable to those in the native cartilage tissue. Moreover, ECM were found to be widely distributed in a network-like structure therein after 12 weeks. The chondrocytes/hydrogel constructs have been developed into a structure with improved mechanical properties and typical cartilage morphology. In the osteochondral defect model, newly formed hyaline cartilage was observed to be integrated with the host articular cartilage tissue in the defect region implanted with chondrocytes/hydrogel constructs at 12 weeks post-surgery. The current experimental result could be further applied to the 4 + 2 system where a mechanically strong hydrogel is needed using various crosslinking chemistry, including changing the end functionality of the star PEG, incorporation of stimuli-responsibility and bioactive factors to the linear linkers.

Acknowledgements

The financial support of the National Natural Science Foundation of China Projects (51273091, 81130034), the Ministry of Science and Technology of China Key Project (2012CB933802), and the Hong Kong Special Administration Region Earmarked Projects (CUHK4042/13P, 2130349/4053060, CUHK7/CRF/12G, 2390062 and GRF14121815) and Guangdong Science and Technology Bureau Project (2013B051000062) are acknowledged.

References

[1] M. Ulrich-Vinther, M.D. Maloney, E.M. Schwarz, R. Rosier, R.J. O'Keefe, Articular cartilage biology, J. Am. Acad. Orthop. Surg. 11 (6) (2003) 421–430.
[2] B.V. Sridhar, J.L. Brock, J.S. Silver, J.L. Leight, M.A. Randolph, K.S. Anseth, Development of a cellularly degradable PEG hydrogel to promote articular cartilage extracellular matrix deposition, Adv. Healthc. Mater 4 (2015) 702–713.
[3] K. Mithoefer, T. McAdams, R.J. Williams, P.C. Kreuz, B.R. Mandelbaum, Clinical efficacy of the microfracture technique for articular cartilage repair in the knee: an evidence-based systematic analysis, Am. J. Sport Med. 37 (10) (2009) 2053–2063.
[4] K. Pelttari, E. Steck, W. Richter, The use of mesenchymal stem cells for chondrogenesis, Injury 39 (2008) S58–S65.
[5] P.B. Lewis, L.P. McCarty III, R.W. Kang, B.J. Cole, Basic science and treatment options for articular cartilage injuries, J. Orthop. Sports Phys. Ther. 36 (10) (2006) 717–727.
[6] R.R. Bannuru, N.S. Natov, I.E. Obadan, L.L. Price, C.H. Schmid, T.E. McAlindon, Therapeutic trajectory of hyaluronic acid versus corticosteroids in the treatment of knee osteoarthritis: a systematic review and meta-analysis, Arthritis Care Res. 61 (12) (2009) 1704–1711.
[7] C. Chung, J.A. Burdick, Engineering cartilage tissue, Adv. Drug Del. Rev. 60 (2) (2008) 243–262.
[8] D. Nesic, R. Whiteside, M. Brittberg, D. Wendt, I. Martin, P. Mainil-Varlet, Cartilage tissue engineering for degenerative joint disease, Adv. Drug Del. Rev. 58 (2) (2006) 300–322.
[9] E. Kon, G. Filardo, B. Di Matteo, F. Perdisa, M. Marcacci, Matrix assisted autologous chondrocyte transplantation for cartilage treatment: a systematic review, Bone Jt. Res. 2 (2) (2013) 18–25.
[10] U. Meyer, T. Meyer, H.P. Wiesmann, Bone and Cartilage Engineering, Springer Science & Business Media, 2006.
[11] C. Vinatier, D. Mrugala, C. Jorgensen, J. Guicheux, D. Noel, Cartilage engineering: a crucial combination of cells, biomaterials and biofactors, Trends Biotechnol. 27 (5) (2009) 307–314.
[12] B.V. Slaughter, S.S. Khurshid, O.Z. Fisher, A. Khademhosseini, N.A. Peppas, Hydrogels in regenerative medicine, Adv. Mater 21 (32–33) (2009) 3307–3329.
[13] D.L. Alge, M.A. Azagarsamy, D.F. Donohue, K.S. Anseth, Synthetically tractable click hydrogels for three-dimensional cell culture formed using tetrazine–norbornene chemistry, Biomacromolecules 14 (4) (2013) 949–953.
[14] S. Yan, T. Wang, L. Feng, J. Zhu, K. Zhang, X. Chen, L. Cui, J. Yin, Injectable in situ self-cross-linking hydrogels based on poly(L-glutamic acid) and alginate for cartilage tissue engineering, Biomacromolecules 15 (12) (2014) 4495–4508.
[15] F. Yu, X. Cao, Y. Li, L. Zeng, B. Yuan, X. Chen, An injectable hyaluronic acid/PEG hydrogel for cartilage tissue engineering formed by integrating enzymatic crosslinking and Diels-Alder "click chemistry", Polym. Chem. 5 (3) (2014) 1082–1090.
[16] Y. Jiang, J. Chen, C. Deng, E.J. Suuronen, Z. Zhong, Click hydrogels, microgels and nanogels: emerging platforms for drug delivery and tissue engineering, Biomaterials 35 (18) (2014) 4969–4985.
[17] M. Lutolf, J. Lauer-Fields, H. Schmoekel, A. Metters, F. Weber, G. Fields, J. Hubbell, Synthetic matrix metalloproteinase-sensitive hydrogels for the conduction of tissue regeneration: engineering cell-invasion characteristics, Proc. Natl. Acad. Sci. U. S. A. 100 (9) (2003) 5413–5418.
[18] M.P. Lutolf, G.P. Raeber, A.H. Zisch, N. Tirelli, J.A. Hubbell, Cell-responsive synthetic hydrogels, Adv. Mater 15 (11) (2003) 888–892.
[19] Y. Park, M.P. Lutolf, J.A. Hubbell, E.B. Hunziker, M. Wong, Bovine primary chondrocyte culture in synthetic matrix metalloproteinase-sensitive poly (ethylene glycol)-based hydrogels as a scaffold for cartilage repair, Tissue Eng. 10 (3–4) (2004) 515–522.
[20] S.J. Bryant, K.S. Anseth, The effects of scaffold thickness on tissue engineered cartilage in photocrosslinked poly(ethylene oxide) hydrogels, Biomaterials 22 (6) (2001) 619–626.
[21] J.A. Burdick, K.S. Anseth, Photoencapsulation of osteoblasts in injectable RGD-modified PEG hydrogels for bone tissue engineering, Biomaterials 23 (22) (2002) 4315–4323.
[22] S.J. Bryant, K.S. Anseth, D.A. Lee, D.L. Bader, Crosslinking density influences the morphology of chondrocytes photoencapsulated in PEG hydrogels during the application of compressive strain, J. Orth. Res. 22 (5) (2004) 1143–1149.
[23] S.J. Bryant, R.J. Bender, K.L. Durand, K.S. Anseth, Encapsulating chondrocytes in degrading PEG hydrogels with high modulus: engineering gel structural changes to facilitate cartilaginous tissue production, Biotechnol. Bioeng. 86 (7) (2004) 747–755.
[24] D.L. Elbert, A.B. Pratt, M.P. Lutolf, S. Halstenberg, J.A. Hubbell, Protein delivery from materials formed by self-selective conjugate addition reactions, J. Control. Release 76 (1–2) (2001) 11–25.
[25] C. Hiemstra, L.J. van der Aa, Z. Zhong, P.J. Dijkstra, J. Feijen, Rapidly in situ-forming degradable hydrogels from dextran thiols through Michael addition, Biomacromolecules 8 (5) (2007) 1548–1556.
[26] P.D. Dalton, C. Hostert, K. Albrecht, M. Moeller, J. Groll, Structure and properties of urea-crosslinked star poly[(ethylene oxide)-ran-(propylene oxide)] hydrogels, Macromol. Biosci. 8 (10) (2008) 923–931.
[27] R. Jin, L.S. Moreira Teixeira, A. Krouwels, P.J. Dijkstra, C.A. van Blitterswijk, M. Karperien, J. Feijen, Synthesis and characterization of hyaluronic acid–poly(ethylene glycol) hydrogels via Michael addition: an injectable biomaterial for cartilage repair, Acta Biomater. 6 (6) (2010) 1968–1977.
[28] S. Moeinzadeh, D. Barati, X. He, E. Jabbari, Gelation characteristics and osteogenic differentiation of stromal cells in inert hydrolytically degradable micellar polyethylene glycol hydrogels, Biomacromolecules 13 (7) (2012) 2073–2086.
[29] K.M. Mabry, R.L. Lawrence, K.S. Anseth, Dynamic stiffening of poly(ethylene glycol)-based hydrogels to direct valvular interstitial cell phenotype in a three-dimensional environment, Biomaterials 49 (2015) 47–56.
[30] J.L. Leight, E.Y. Tokuda, C.E. Jones, A.J. Lin, K.S. Anseth, Multifunctional biocaffolds for 3D culture of melanoma cells reveal increased MMP activity and migration with BRAF kinase inhibition, Proc. Natl. Acad. Sci. U. S. A. 112 (17) (2015) 5366–5371.
[31] B.V. Sridhar, N.R. Doyle, M.A. Randolph, K.S. Anseth, Covalently tethered TGF-β1 with encapsulated chondrocytes in a PEG hydrogel system enhances extracellular matrix production, J. Biomed. Mater. Res. A 102 (12) (2014) 4464–4472.
[32] N. Yamaguchi, L. Zhang, B.-S. Chae, C.S. Palla, E.M. Furst, K.L. Kiick, Growth factor mediated assembly of cell receptor-responsive hydrogels, J. Am. Chem. Soc. 129 (11) (2007) 3040–3041.
[33] C.A. DeForest, B.D. Polizzotti, K.S. Anseth, Sequential click reactions for synthesizing and patterning three-dimensional cell microenvironments, Nat.

Mater 8 (8) (2009) 659–664.
[34] C.A. DeForest, K.S. Anseth, Cytocompatible click-based hydrogels with dynamically tunable properties through orthogonal photoconjugation and photocleavage reactions, Nat. Chem. 3 (12) (2011) 925–931.
[35] J.E. Mark, B. Erman, Rubberlike Elasticity: a Molecular Primer, Cambridge University Press, 2007.
[36] D. Eyrich, F. Brandl, B. Appel, H. Wiese, G. Maier, M. Wenzel, R. Staudenmaier, A. Goepferich, T. Blunk, Long-term stable fibrin gels for cartilage engineering, Biomaterials 28 (1) (2007) 55–65.
[37] T. Iwao, Polymer Solutions: an Introduction to Physical Properties, Wiley, New York, 2002.
[38] G. Wang, X. Fan, B. Hu, Y. Zhang, J. Huang, Synthesis of eight-shaped poly(-ethylene oxide) by the combination of glaser coupling with ring-opening polymerization, Macromol. Rapid Commun. 32 (20) (2011) 1658–1663.
[39] M.P. Lutolf, J.A. Hubbell, Synthesis and physicochemical characterization of end-linked poly(ethylene glycol)-co-peptide hydrogels formed by Michael-type addition, Biomacromolecules 4 (3) (2003) 713–722.
[40] B. Chu, Laser Light Scattering: Basic Principles and Practice, Acad. Press, 1991.
[41] C. Wu, M. Siddiq, K.F. Woo, Laser light scattering characterization of a polymer mixture made of individual linear chains and clusters, Macromolecules 28 (14) (1995) 4914–4919.
[42] C. Wu, S. Zhou, Internal motions of both poly(N-isopropylacrylamide) linear chains and spherical microgel particles in water, Macromolecules 29 (5) (1996) 1574–1578.
[43] B.J. Berne, R. Pecora, Dynamic Light Scattering: with Applications to Chemistry, Biology, and Physics, Courier Dover Publications, 2000.
[44] J. Li, T. Ngai, C. Wu, The slow relaxation mode: from solutions to gel networks, Polym. J. 42 (8) (2010) 609–625.
[45] F. Jin, J. Ye, L.Z. Hong, H.F. Lam, C. Wu, Slow relaxation mode in mixtures of water and organic molecules: supramolecular structures or nanobubbles? J. Phys. Chem. B 111 (9) (2007) 2255–2261.
[46] F. Jin, X. Ye, C. Wu, Observation of kinetic and structural scalings during slow coalescence of nanobubbles in an aqueous solution, J. Phys. Chem. B 111 (46) (2007) 13143–13146.
[47] J. Wang, The origin of the slow mode in dilute aqueous solutions of PEO, Macromolecules 48 (5) (2015) 1614–1620.
[48] M. Chen, A.C. Lichtler, T.-J. Sheu, C. Xie, X. Zhang, R.J. O'Keefe, D. Chen, Generation of a transgenic mouse model with chondrocyte-specific and tamoxifen-inducible expression of Cre recombinase, Genesis 45 (1) (2007) 44–50.
[49] F. Zhang, Q. He, W.P. Tsang, W.T. Garvey, W.Y. Chan, C. Wan, Insulin exerts direct, IGF-1 independent actions in growth plate chondrocytes, Bone Res. 2 (2014) 14012.
[50] P. Wang, F. Zhang, Q. He, J. Wang, H.T. Shiu, Y. Shu, W.P. Tsang, S. Liang, K. Zhao, C. Wan, Flavonoid compound icariin activates hypoxia inducible factor-1? in chondrocytes and promotes articular cartilage repair, PLoS One 11 (2) (2016) e0148372.
[51] J.-L. Ruan, N.L. Tulloch, V. Muskheli, E.E. Genova, P.D. Mariner, K.S. Anseth, C.E. Murry, An improved cryosection method for polyethylene glycol hydrogels used in tissue engineering, Tissue Eng. Part C Methods 19 (10) (2013) 794–801.
[52] A. Forni, F. Ganazzoli, M. Vacatello, Molecular shape of regular star polymers by Monte Carlo simulations, Macromolecules 30 (16) (1997) 4737–4743.
[53] T. Sakai, T. Matsunaga, Y. Yamamoto, C. Ito, R. Yoshida, S. Suzuki, N. Sasaki, M. Shibayama, U.I. Chung, Design and fabrication of a high-strength hydrogel with ideally homogeneous network structure from tetrahedron-like macromonomers, Macromolecules 41 (14) (2008) 5379–5384.
[54] T.A. Witten, P.A. Pincus, M.E. Cates, Macrocrystal ordering in star polymer solutions, Europhys. Lett. 2 (2) (1986) 137–140.
[55] D. Richter, O. Jucknischke, L. Willner, L.J. Fetters, M. Lin, J.S. Huang, J. Roovers, C. Toporovski, L.L. Zhou, Scaling properties and ordering phenomena of star polymers in solution, J. Phys. IV 3 (C8) (1993) 3–12.
[56] Q. Ying, B. Chu, Overlap concentration of macromolecules in solution, Macromolecules 20 (2) (1987) 362–366.
[57] W. Brown, T. Nicolai, Static and dynamic behavior of semidilute polymer solutions, Colloid. Polym. Sci. 268 (11) (1990) 977–990.
[58] I. Teraoka, Polymer Solutions: an Introduction to Physical Properties, Wiley, 2002.
[59] J.F. Li, W. Li, H. Huo, S.Z. Luo, C. Wu, Reexamination of the slow mode in semidilute polymer solutions: the effect of solvent quality, Macromolecules 41 (3) (2008) 901–911.
[60] B. Chu, Static and dynamic properties of polymer solutions, in: S.-H. Chen, B. Chu, R. Nossal (Eds.), Scattering Techniques Applied to Supramolecular and Nonequilibrium Systems, Springer, US, 1981, pp. 231–264.
[61] Z. Wang, B. Chu, Q. Wang, L. Fetters, Diffusion of polymer in binary and ternary semidilute solutions, in: L.-H. Lee (Ed.), New Trends in Physics and Physucal Chemistry of Polymers, Springer, US, 1989, pp. 207–228.
[62] K. Huber, S. Bantle, W. Burchard, L.J. Fetters, Semidilute solutions of star branched polystyrene: a light and neutron scattering study, Macromolecules 19 (5) (1986) 1404–1411.
[63] J. Wang, C. Wu, Reexamination of the origin of slow relaxation in semidilute polymer solutions—reptation related or not? Macromolecules 49 (8) (2016) 3184–3191.
[64] P. Wiltzius, H.R. Haller, D.S. Cannell, D.W. Schaefer, Dynamics of long-wavelength concentration fluctuations in solutions of linear-polymers, Phys. Rev. Lett. 53 (8) (1984) 834–837.
[65] D.J. Huey, J.C. Hu, K.A. Athanasiou, Unlike bone, cartilage regeneration remains elusive, Science 338 (6109) (2012) 917–921.
[66] R. von Eisenhart, C. Adam, M. Steinlechner, M. Müller-Gerbl, F. Eckstein, Quantitative determination of joint incongruity and pressure distribution during simulated gait and cartilage thickness in the human hip joint, J. Orth. Res. 17 (4) (1999) 532–539.
[67] L.A. Smith Callahan, A.M. Ganios, E.P. Childers, S.D. Weiner, M.L. Becker, Primary human chondrocyte extracellular matrix formation and phenotype maintenance using RGD-derivatized PEGDM hydrogels possessing a continuous Young's modulus gradient, Acta Biomater. 9 (4) (2013) 6095–6104.
[68] A.K. Williamson, A.C. Chen, R.L. Sah, Compressive properties and function-composition relationships of developing bovine articular cartilage, J. Orth. Res. 19 (6) (2001) 1113–1121.
[69] K.A. Athanasiou, M.P. Rosenwasser, J.A. Buckwalter, T.I. Malinin, V.C. Mow, Interspecies comparisons of in situ intrinsic mechanical properties of distal femoral cartilage, J. Orth. Res. 9 (3) (1991) 330–340.
[70] F. Guilak, W.R. Jones, H.P. Ting-Beall, G.M. Lee, The deformation behavior and mechanical properties of chondrocytes in articular cartilage, Osteoarthr. Cartil. 7 (1) (1999) 59–70.
[71] L.G. Alexopoulos, G.M. Williams, M.L. Upton, L.A. Setton, F. Guilak, Osteoarthritic changes in the biphasic mechanical properties of the chondrocyte pericellular matrix in articular cartilage, J. Biomech. 38 (3) (2005) 509–517.
[72] E.M. Darling, R.E. Wilusz, M.P. Bolognesi, S. Zauscher, F. Guilak, Spatial mapping of the biomechanical properties of the pericellular matrix of articular cartilage measured in situ via atomic force microscopy, Biophys. J. 98 (12) (2010) 2848–2856.
[73] H. Akiyama, M.C. Chaboissier, J.F. Martin, A. Schedl, B. de Crombrugghe, The transcription factor Sox9 has essential roles in successive steps of the chondrocyte differentiation pathway and is required for expression of Sox5 and Sox6, J. Bone Min. Res. 17 (2002) S142.
[74] J. Elisseeff, Injectable cartilage tissue engineering, Expert Opin. Biol. Ther. 4 (12) (2004) 1849–1859.
[75] F. Wolf, C. Candrian, D. Wendt, J. Farhadi, M. Heberer, I. Martin, A. Barbero, Cartilage tissue engineering using pre-aggregated human articular chondrocytes, Eur. Cell Mater 16 (2008) 92–99.
[76] S. Strobel, M. Loparic, D. Wendt, A.D. Schenk, C. Candrian, R. Lindberg, F. Moldovan, A. Barbero, I. Martin, Anabolic and catabolic responses of human articular chondrocytes to varying oxygen percentages, Arthritis Res. Ther. 12 (2) (2010) R34.
[77] C.-Y. Ko, C.-Y. Yang, S.-R. Yang, K.-L. Ku, C.-K. Tsao, D. Chwei-Chin Chuang, I.M. Chu, M.-H. Cheng, Cartilage formation through alterations of amphiphilicity of poly(ethylene glycol)-poly(caprolactone) copolymer hydrogels, RSC Adv. 3 (48) (2013) 25769–25779.